

Research Article

Effect of Modifying Prosthetic Socket Base Materials by Adding Nanodiamonds

Lifang Ma,^{1,2} Xiaogang Hu,³ Shizhong Zhang,¹ and Yu Chen¹

¹Beijing Institute of Technology, Beijing 100081, China

²National Research Center for Rehabilitation Technical Aids, Beijing 100176, China

³Beijing Grish Hitech Co., Ltd., Beijing 100085, China

Correspondence should be addressed to Lifang Ma; malifang@sohu.com

Received 23 September 2014; Accepted 19 November 2014

Academic Editor: Jumin Hao

Copyright © 2015 Lifang Ma et al. This is an open access article distributed under the Creative Commons Attribution License, which permits unrestricted use, distribution, and reproduction in any medium, provided the original work is properly cited.

The curing process of prosthetic socket base materials requires attention owing to a series of associated problems that are yet to be addressed and solved. However, to date, few relevant studies have been reported. In this paper, nanodiamonds modified with a silane coupling agent were dispersed into a prosthetic socket base material, and the performance of the modified base materials was investigated. Adding a predetermined amount of nanodiamonds to the prosthetic socket base material increased the glass transition temperature, improved the mechanical properties of the cured base material, and reduced the influence of the volatile gas formed during the curing process on the environment. With increasing nanodiamond contents, the glass transition temperature increased and the mechanical properties improved slightly. Owing to the high thermal conductivity of the nanodiamonds, the localized heat, as a result of the curing process, could be dissipated and released. Thus, adding nanodiamonds led to a more uniform temperature field forming in the curing system. This improved the curing process and reduced the formation of volatile monomers, thereby decreasing the adverse impact of the generated volatile gases on the environment. All of these provide a potential strategy for modifying prosthetic socket base materials.

1. Introduction

A prosthesis is an artificial limb that is produced and assembled to restore the human body form and function and compensate for deficiencies caused by amputation. The installation of a prosthesis is a crucial step for the rehabilitation and reintegration of the amputee into society. The prosthetic socket is an important part that connects the patient's stump to the prosthesis and thus plays an important role in determining the performance of the prosthesis. However, to date, studies on prosthetic socket materials, particularly their preparation and characterization, are rarely reported.

The most common base materials employed for prosthetic sockets are modified poly(methyl methacrylate)-based fiber composite materials fabricated in a two-step process. The first step involves using methyl methacrylate (MMA) monomers to synthesize prepolymers and subsequently generating a modified base material for prosthetic socket

fabrication. The second step involves curing the modified base material and fiber material at ambient temperature to obtain the prosthetic socket. The performance of the base material plays a very important role in the following process for obtaining a comfortable, wearable prosthetic socket.

Currently, there are some problems associated with preparing prosthetic socket base materials such as instability of the curing process under ambient temperature, the occurrence of localized heat during the curing process, and related difficulties in heat release. Because the curing reaction of the base material is exothermic, localized heat concentration typically occurs during the curing process. Consequently, this instigates a high internal thermal stress in the base material, causing voids and cracks to form, thereby reducing the performance of the prosthetic socket material. This phenomenon is usually attributed to the poor thermal conductivity of the base material [1, 2]. During the curing process, the localized heating rate is high and heat release is

difficult, thereby generating a nonuniform temperature field in the curing system. Extremely high local temperatures can also result in increased volatility of the MMA monomer in the base material—MMA is a volatile and colorless gas with a pungent smell—causing adverse effects on the working environment during the curing reaction [3, 4].

Currently, several studies have been reported which focus on the improvement of the thermal conductivity of resin materials through the addition of nanoparticles [5, 6]. However, these studies mainly focus on the overall thermal conductivity of the prepared material and ignore the release of localized heat in the socket material during the curing process. Nanodiamonds exhibit excellent biocompatibility and mechanical and thermal conducting properties, and numerous studies have reported the preparation of nanodiamond-resin composite materials [7–16]. However, using nanodiamonds to improve the curing process of prosthetic sockets remains unexplored. In this paper, modified nanodiamonds were dispersed into the prosthetic socket base material, and the effect of the nanodiamonds on the curing process and performance of the cured base material was studied. In particular, the formation of volatile gases during the curing process and their influence on the environment were examined. The influence of volatile gases on the properties of the cured base material was also investigated.

2. Experimental Section

2.1. Materials. MMA, benzoyl peroxide (BPO), and *N,N*-dimethylaniline were obtained from Tianjin Fuchen Chemical Reagent Factory (Tianjin, China). Prior to the experiments, MMA was purified by vacuum distillation. The dicyclohexyl phthalate esters were purchased from Sinopharm Chemical Reagent Co., Ltd. (Tianjin, China), and phenyl salicylate was obtained from Beijing Hengye Zhongyuan Chemical Co. (Beijing, China). Nanodiamonds modified with a silane coupling agent were obtained from Beijing Guoruisheng Technology Co., Ltd. (Beijing, China).

2.2. Methods

2.2.1. Preparation of the Base Material. A four-neck flask was used as the polymerization reactor, which was equipped with an electric stirrer, a thermometer, a reflux condenser, and a nitrogen inlet. MMA (97.5 wt.%), BPO (0.5 wt.%), dicyclohexyl phthalate ester (0.75 wt.%), and phenyl salicylate (0.75 wt.%) were added to the flask to initiate polymerization at 70°C in a dry nitrogen atmosphere for 20–25 minutes. Following cooling of the resulting prepolymer to room temperature, *N,N*-dimethylaniline (0.7 wt.%), saccharin (0.2 wt.%), and the inhibitor (0.1 wt.%) were added, and the base material was obtained after thoroughly mixing the material.

2.2.2. Modification of the Base Material with Nanodiamonds. Our previous modification experiments showed that nanodiamond particles were readily precipitated from the base material when the nanodiamond content was above 1 wt.%. Therefore, in this study, the nanodiamond content was varied between 0 and 1 wt.%. The base material was evenly mixed

with different contents of nanodiamonds (0.1, 0.2, 0.3, 0.5, 0.75, and 1 wt.%) using sonication and a defoaming machine. The resulting product was filtered with a sieve to obtain the modified base material.

2.2.3. Curing Reaction at Room Temperature. The curing agent was added to the base material at room temperature, simulating the actual preparation and processing conditions employed for prosthetic sockets.

2.3. Sample Characterization

2.3.1. Fourier Transform Infrared Spectroscopy (FTIR). For sample preparation, pellets were prepared by mixing the matrix material with KBr. The pellet was then characterized using a Shimadzu Iffinity-21 Fourier transform infrared spectrophotometer. The resolution was set to 4 cm⁻¹ and the scan number to 16.

2.3.2. Differential Scanning Calorimetry. A Shimadzu DSC-60 differential scanning calorimetry (DSC) apparatus was used to determine the glass transition temperature of the base material in the temperature range from -250°C to -50°C at a heating rate of 10°C min⁻¹. The sample mass used for analysis was between 5 and 8 mg. For the DSC experiments, nitrogen was used as a protective gas at a flow rate of 30 mL min⁻¹.

2.3.3. Evaluation of the Mechanical Properties of the Base Materials. An in-house-built WDT-type universal testing machine was used to measure the flexural strength and elastic modulus of the samples. Three-point bending tests with a specimen span of 34 mm and a loading speed of 5 mm min⁻¹ were performed according to the GB/T 1449-2005 standard. A domestic HXD-TM-type microhardness tester was used to measure the microhardness of the cured material.

2.3.4. Determination of the Curing Peak Temperature of the Reaction System. The curing agent was mixed with 50 g of the base material and stirred to obtain a uniform mixture. The mixture, contained in a tube, was then placed in a water bath equipped with a thermometer at a set temperature. The SPI method was used as a reference for the temperature measurements. Owing to the specific technical requirements of the prosthetic socket preparation process, the temperature of the water bath was controlled at 25°C.

2.3.5. Determination of the Concentration of MMA in Air during the Curing Process [3, 4]. The concentration of MMA in air during the curing process was determined by gas chromatography. The volatilized MMA in the air was collected by activated carbon contained in a tube. Methanol solution was used for desorption and a 5% PEG-6000-containing column was used for separation. A hydrogen flame ionization detector was used to measure the concentration of MMA in the air during the curing process.

2.3.6. Electron Microscopy Analysis. Prior to analysis, the samples were quenched in liquid nitrogen for 30 min to allow

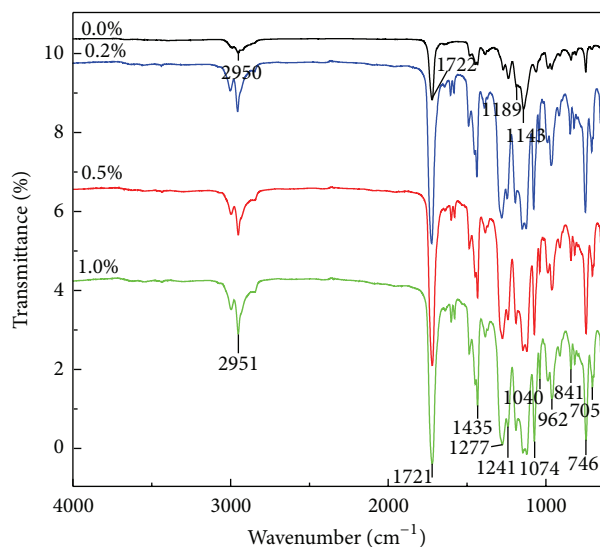


FIGURE 1: FTIR spectra of the cured base materials prepared with varying nanodiamond contents.

cracks to form. After being coated with gold, the samples were investigated by scanning electron microscopy (Hitachi S-4800) on a microscope operating at an acceleration voltage of 20 kV. Transmission electron microscopy analysis was then performed on slices of the samples on an FEI 300 kV field-emission transmission electron microscope.

3. Results and Discussion

3.1. FTIR Spectra of the Cured Base Materials. After the curing reaction of the nanodiamonds-containing base materials was completed, the base materials were characterized by FTIR spectroscopy. Figure 1 shows the FTIR spectra of the cured base materials prepared with varying nanodiamond contents. The broad absorption peak at 2950 cm^{-1} was attributed to the symmetric and antisymmetric stretching vibrations of the C–H bonds in the $-\text{CH}_3$ and $-\text{CH}_2-$ groups. After the nanodiamonds were added, the intensity of the peak (2950 cm^{-1}) increased and became broader because of the existing silane coupling agent in the nanodiamonds. The peaks corresponding to C–C–O–C stretching vibrations at 1143, 1189, 1241, and 1277 cm^{-1} were similar to the characteristic bands of PMMA, whereas the intensity of the peaks at 1435 and 1277 cm^{-1} substantially increased, confirming the deformation vibration of the Si– CH_2 bonds. Additionally, the intensity of the C=O stretching vibration absorption peak at 1722 cm^{-1} increased with increasing nanodiamond contents.

Absorption peaks in the range $700\text{--}900\text{ cm}^{-1}$ were attributed to the stretching vibration of the Si–C bond. The peak at 962 cm^{-1} was attributed to the stretching vibration of the Si–O–C bond, and that at 1040 cm^{-1} was attributed to the stretching vibration of the Si–O–Si bond. The presence of these peaks confirmed the existence of the silane coupling agent, thereby indicating that it was successfully grafted to the surface of the nanodiamonds through Si–O–C bonds [10].

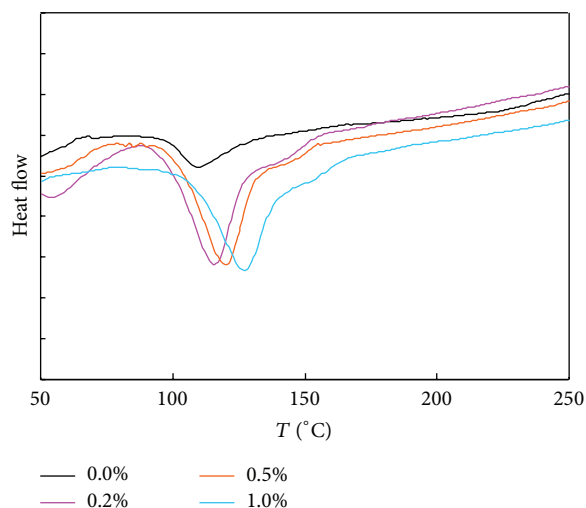


FIGURE 2: DSC curves of the base material containing varying amounts of nanodiamonds.

In summary, FTIR analysis revealed that the silane coupling agent molecules grafted to the surface of the nanodiamonds through hydrogen bonds. Additionally, self-polymerization of the silane coupling agent molecules led to the formation of Si–O–Si bonds and a layered network structure. The hydroxyl groups on the surface of the base material may indirectly combine with the nanodiamond particles via hydrogen bonding between the hydroxyl groups and the carbonyl groups of the silane coupling agent molecules [9, 10].

3.2. Glass Transition Temperature of the Cured Base Material. Figure 2 shows that the glass transition temperature (T_g) of the base material gradually increased with increasing nanodiamond content. Nanodiamonds modified with the silane coupling agent could be better dispersed in the base material because of their small size. This would enhance the interaction between the macromolecules through interactions between the polar groups in the macromolecular PMMA chains of the base material and those in the silane coupling agent grafted to the nanodiamond surface. However, the added nanodiamonds occupied the void spaces between the macromolecules, thus inhibiting the movement of the macromolecular chains. These two factors led to a significant increase in the activation energy associated with the movement of the PMMA segment in the base material, resulting in increased glass transition temperatures.

3.3. Mechanical Properties of the Cured Base Material. Table 1 shows the mechanical properties of the base material prepared with varying amounts of nanodiamonds. The cured nanodiamond-containing base materials displayed slightly improved mechanical properties. The slight improvement was mainly due to the larger steric hindrance and stronger interactions between the modified nanodiamonds and the macromolecules in the base material. Consequently, the modified nanodiamonds were more stable in the base

TABLE 1: Mechanical properties of the cured base material prepared with varying nanodiamond contents.

Nanodiamond content (wt.%)	Compression strength	Tensile strength (MPa)	Elastic modulus (MPa)	Microhardness
0.0	73.46 ± 1.56	39.23 ± 1.69	980.75 ± 78.38	9.17
0.2	74.20 ± 1.07	39.86 ± 1.35	1017.43 ± 52.12	10.53
0.5	77.55 ± 1.90	43.47 ± 1.21	1123.87 ± 28.71	13.15
1.0	79.32 ± 1.88	44.91 ± 1.39	1198.62 ± 48.40	13.29

materials. After the curing agent was added, the interaction between the silane coupling agent molecules on the nanodiamond surface and the C=C double bonds and hydrogen bonds in the substrate molecules was activated. The activated bonds randomly attracted adjacent double bonds and hydrogen bonds to form new chemical bonds that interwove and self-polymerized to generate a three-dimensional network structure. The combination of the nanodiamond particles with the base material via chemical bonds led to enhanced mechanical properties of the cured base material. However, improvement was only marginal because of the low nanodiamond content.

3.4. Temperature Change in the Curing Reaction of the Base Materials. Owing to the technical requirements of the prosthetic socket preparation process, the base material should exhibit long-term stability for storage, whereas the curing reaction, once initiated, must be promptly completed under normal temperature. The curing reaction of the prosthetic socket base material mainly involves reaction of the PMMA prepolymers initiated by *N,N*-dimethylaniline and BPO. *N,N*-Dimethylaniline is a catalyst towards promoting the activity of BPO. The O–O bond in BPO decomposes to form two active groups, which react with the PMMA prepolymer, breaking the C=C double bonds and initiating further polymerization of the prepolymers. During the polymerization process, part of the *N,N*-dimethylaniline generates active nitrogen radicals that can initiate polymerization of the prepolymer. Both the high heating rate and relatively high viscosity of the prepolymers lead to the generation of localized curing heat, which is difficult to dissipate, thus creating a nonuniform temperature field in the system. In particular, bubbles resulting from the evaporation of unreacted MMA monomers will form under a local high temperature. All of these factors have a direct impact on the performance and future usability of the prosthetic socket material.

Figure 3 shows the change in the temperature in the reaction system following the addition of the curing agent to the base materials with different nanodiamond content. With increasing nanodiamond content, the peak temperature during the curing reaction of the base material gradually decreased. At a nanodiamond content of 1 wt.%, the peak temperature decreased by more than 10 °C. Therefore, adding nanodiamonds is an effective means of reducing the peak temperature and increasing the uniformity of the curing system temperature field. Concurrently, the number of bubbles generated during the curing process is reduced.

3.5. Determination of Monomer Content in Air during the Curing Reaction. MMA is a volatile and colorless gas with a

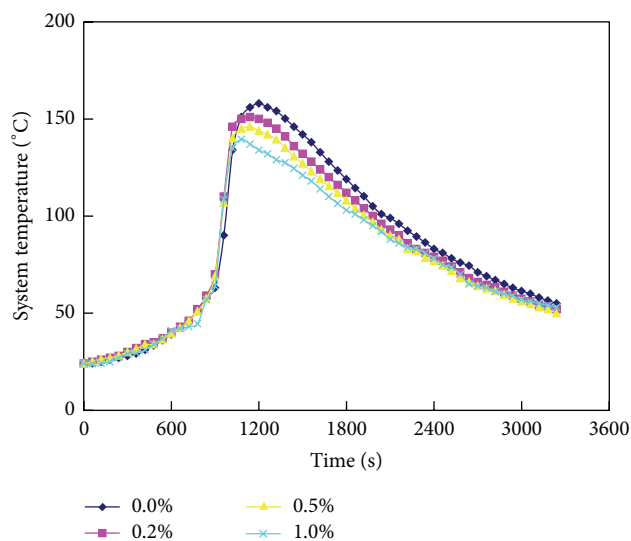


FIGURE 3: Temperature associated with the curing reaction of the base materials prepared with varying nanodiamond contents.

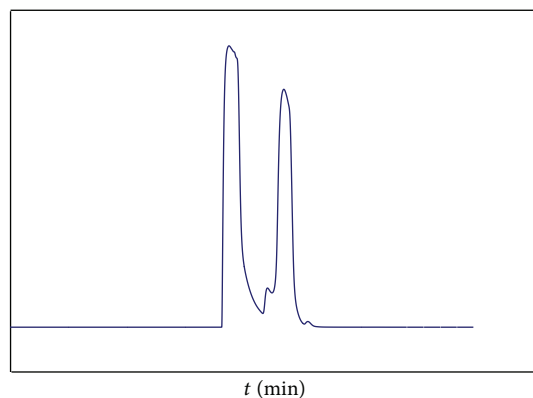


FIGURE 4: Chromatogram of methanol and methyl methacrylate.

pungent odor. Long-term exposure to poly-MMA can lead to chronic poisoning in humans, posing serious health hazards. The main health hazard is damage to the nervous system; in rare cases, exposure may cause toxic encephalopathy or teratogenesis. Additionally, MMA has some carcinogenic characteristics [3, 4]. Thus, any unreacted MMA monomers in the prosthetic socket base material are very likely to volatilize under local high temperatures, and the residual MMA monomers can result in contamination of the working environment. Table 2 lists the content of the MMA monomers in air during the curing process of the base

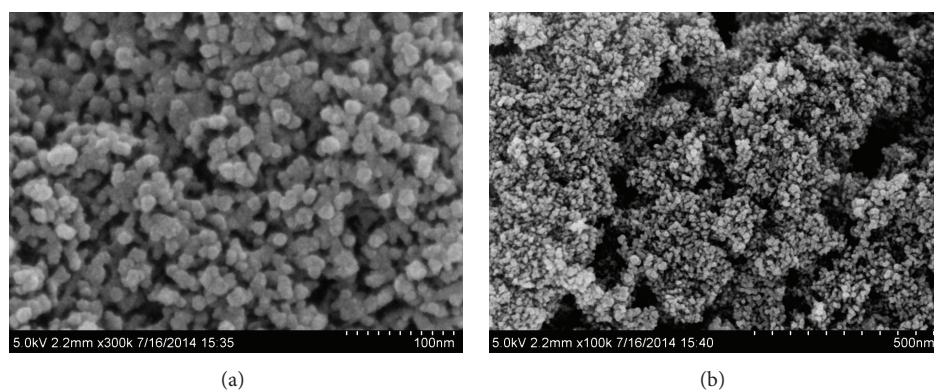


FIGURE 5: Representative scanning electron microscopy images of the modified nanodiamonds.

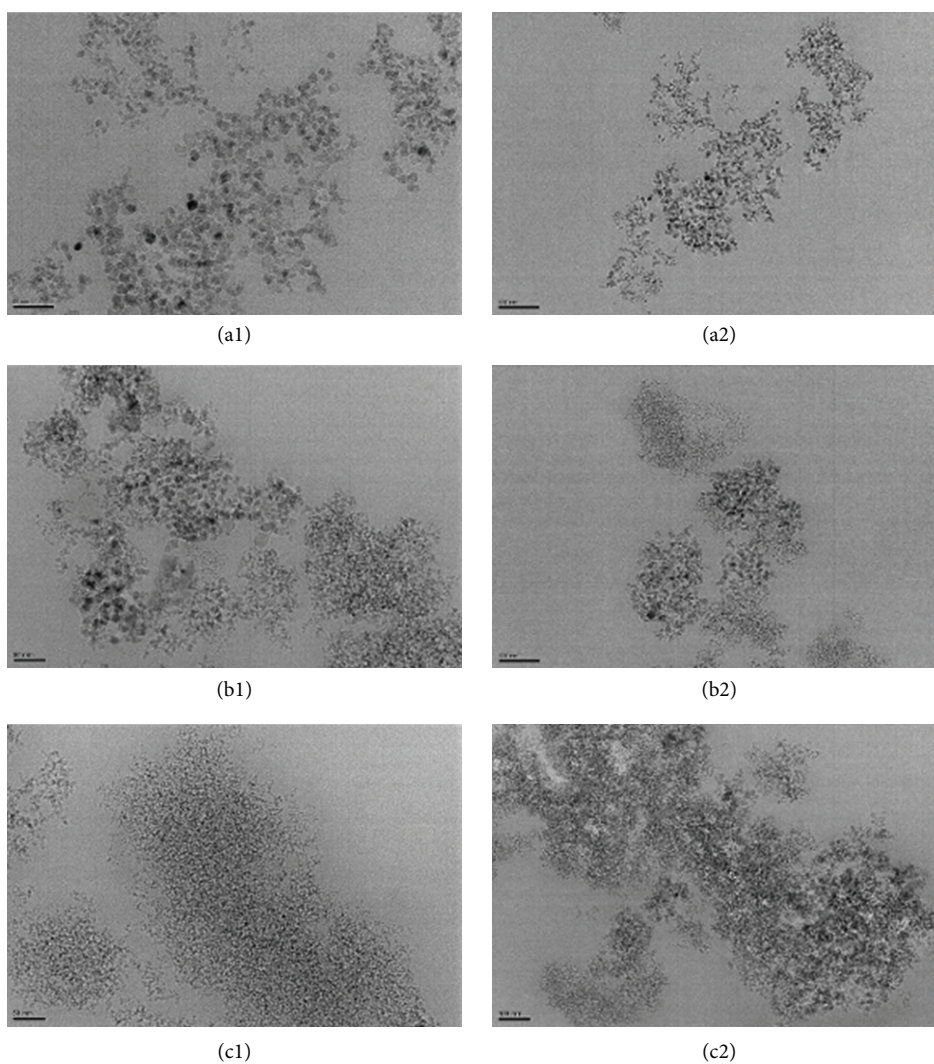


FIGURE 6: Representative transmission electron microscopy images of the nanodiamonds dispersed in the base material at varying contents: (a) 0.2, (b) 0.5, and (c) 1.0 wt.%.

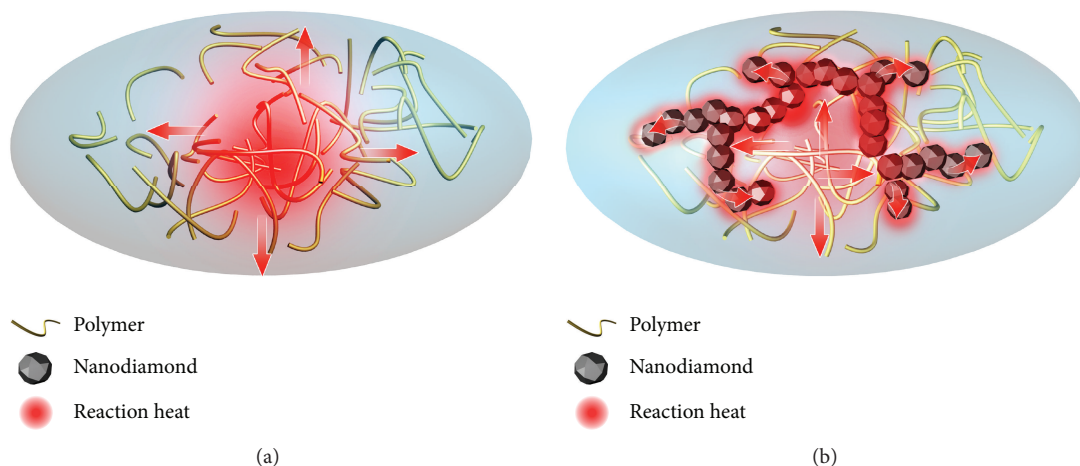


FIGURE 7: Heat dissipation model in the base material in the (a) absence and (b) presence of nanodiamonds.

TABLE 2: Content of MMA monomers in air for the base materials prepared with different nanodiamond contents.

Nanodiamond content (wt.%)	MMA monomer content in air (g/m^3)
0.0	0.337
0.5	0.201
1.0	0.137

materials prepared with varying nanodiamond contents; the associated chromatogram is shown in Figure 4. As observed from Table 2, the amount of volatilized MMA monomers decreased gradually with increase in the nanodiamond content. Therefore, adding nanodiamonds helps to reduce the amount of harmful volatilized gases. This effect can be attributed to the decrease in the local high temperature.

3.6. Electron Microscopy Analysis. Figure 5 shows representative scanning electron microscopy images of the nanodiamonds modified with a silane coupling agent. The nanodiamond particles were spherical with sizes between 5 and 10 nm and no visible edges. The specific surface area of the particles was typically $300\text{--}400\text{ m}^2\text{ g}^{-1}$, with a maximum of $450\text{ m}^2\text{ g}^{-1}$. Figure 6 shows transmission electron microscopy images of the nanodiamonds dispersed in the base material at varying contents. With increasing nanodiamond content, the distribution density of the nanodiamonds in the resin and the probability of occurrence and observed amount of the nanodiamonds increased. At a nanodiamond content of 0.2 wt.%, the nanodiamond particles were more loosely dispersed in the resin, and thus the distance between the particles and agglomerates was larger. When the nanodiamond content exceeded 0.2 wt.%, the amount and volume of the nanodiamond agglomerates significantly increased, thereby leading to reduced separation between the agglomerates [7, 8].

These results showed that the agglomeration of the nanodiamond particles increased with increasing nanodiamond

content. Furthermore, the transmission electron microscopy images revealed that the resin matrix penetrated the gaps between the nanodiamond agglomerates. Consequently, except for the microscopic chemical bonding between the nanodiamond agglomerates and the base resin material, the filling phenomenon resulted in macroscopic physical interactions, such as mechanical interlocking, which strengthened the connection between the diamond agglomerates and the base resin material.

As schematically illustrated in Figure 7, adding nanodiamonds to the base material led to a decrease in the peak temperature during the curing process of the base material. This decrease in temperature is due to the very high thermal conductivity of the nanodiamonds ($\sim 2300\text{ W m}^{-1}\text{ K}^{-1}$). The local distribution of the nanodiamonds in the base material shows some network connections and agglomerates. This network structure can benefit from the nanodiamonds' high thermal diffusivity, which effectively dissipates and releases heat from high-temperature areas, thus reducing differences in the temperature field of the entire system. Therefore, adding nanodiamonds to the base material can improve the curing process and reduce the amount of volatilized monomer and therefore decrease the adverse effects on the environment. The current strategy provides a potential pathway for the processing and modification of prosthetic socket base materials.

4. Conclusions

The current findings show that adding a predetermined amount of nanodiamonds (between 0.1 and 1.0 wt.%) to the prosthetic socket base material can increase the glass transition temperature and improve the mechanical properties of the cured base material. With increasing nanodiamond contents, the glass transition temperature increased and the mechanical properties improved slightly. Owing to the high thermal conductivity of the nanodiamonds, the localized curing reaction heat was dissipated and released, affording a more uniform temperature field in the curing system.


Therefore, adding nanodiamonds can improve the curing process of the base material, reduce the amount of unreacted volatile monomer, and decrease the adverse effects of any unreacted volatile monomer on the working environment. This provides a potential for improving the method and safety for the processing and modification of prosthetic socket base materials.

Conflict of Interests

The authors declare that there is no conflict of interests regarding the publication of this paper.

References

- [1] Q. Wang, T.-W. Wang, and W. Wei, "Study on thickening characteristics and curing behavior of unsaturated polyester resin," *Engineering Plastics Application*, vol. 34, pp. 37–40, 2006.
- [2] X. Li, Y. Yan, and S. Mao, "Determination of storage life and gelation time of UPR," *China Synthetic Resin and Plastics*, vol. 20, no. 1, pp. 24–27, 2003.
- [3] Y.-J. Zhao and Z.-H. Xu, "Study on the determination of methyl methacrylate in air of workplace using solvent desorption gas chromatography," *Chinese Journal of Industrial Medicine*, vol. 23, pp. 152–154, 2010.
- [4] F.-L. Tang and W. Zhu, "Separation and determination of ethyl acrylate and methyl methacrylate in ambient air by gas chromatography," *Analysis and Testing Technology and Instruments*, vol. 6, pp. 115–118, 2000.
- [5] J. Yu, X. Huang, L. Wang et al., "Preparation of hyperbranched aromatic polyamide grafted nanoparticles for thermal properties reinforcement of epoxy composites," *Polymer Chemistry*, vol. 2, no. 6, pp. 1380–1388, 2011.
- [6] R. Qian, J. Yu, L. Xie, Y. Li, and P. Jiang, "Efficient thermal properties enhancement to hyperbranched aromatic polyamide grafted aluminum nitride in epoxy composites," *Polymers for Advanced Technologies*, vol. 24, no. 3, pp. 348–356, 2013.
- [7] Y.-Q. Chu, Y. Tong, F.-L. Huang, and T.-L. Zhang, "Structure and properties of boundary layer between nanodiamond and resin matrix," *Transaction of Beijing Institute of Technology*, vol. 33, no. 1, pp. 1–5, 2013.
- [8] Y.-Q. Chu, Y. Tong, T.-L. Zhang, and F.-L. Huang, "Mechanical properties of dental composite resins containing nanodiamond of different diameters," *Journal of Beijing Institute of Technology*, vol. 21, no. 1, pp. 19–22, 2012.
- [9] Y.-Q. Chu, Y. Tong, T.-L. Zhang, F.-L. Huang, and X.-Z. Wang, "Synthesis of nanodiamond reinforced dental composite resins and their mechanical properties," *Fullerenes, Nanotubes and Carbon Nanostructures*, vol. 20, pp. 628–632, 2012.
- [10] X.-G. Hu, X.-Y. Gu, Y. Tong et al., "Study on modified ultrafine-diamond reinforcing and toughening bis-phenol A dental composites," *New Chemical Materials*, vol. 34, pp. 60–62, 2006.
- [11] W. Yu, H. Xie, Y. Li, L. Chen, and Q. Wang, "Experimental investigation on the thermal transport properties of ethylene glycol based nanofluids containing low volume concentration diamond nanoparticles," *Colloids and Surfaces A: Physicochemical and Engineering Aspects*, vol. 380, no. 1–3, pp. 1–5, 2011.
- [12] H. Xie, W. Yu, and Y. Li, "Thermal performance enhancement in nanofluids containing diamond nanoparticles," *Journal of Physics D: Applied Physics*, vol. 42, Article ID 095413, 2009.
- [13] D. Wang, Y. Tong, Y. Li, Z. Tian, R. Cao, and B. Yang, "PEGylated nanodiamond for chemotherapeutic drug delivery," *Diamond and Related Materials*, vol. 36, pp. 26–34, 2013.
- [14] D.-J. Lim, M. Sim, L. Oh, K. Lim, and H. Park, "Carbon-based drug delivery carriers for cancer therapy," *Archives of Pharmacal Research*, vol. 37, no. 1, pp. 43–52, 2014.
- [15] V. N. Mochalin, A. Pentecost, X.-M. Li et al., "Adsorption of drugs on nanodiamond: toward development of a drug delivery platform," *Molecular Pharmaceutics*, vol. 10, no. 10, pp. 3728–3735, 2013.
- [16] J.-H. Liu, S.-T. Yang, X.-X. Chen, and H. Wang, "Fluorescent carbon dots and nanodiamonds for biological imaging: preparation, application, pharmacokinetics and toxicity," *Current Drug Metabolism*, vol. 13, no. 8, pp. 1046–1056, 2012.



Hindawi

Submit your manuscripts at
<http://www.hindawi.com>

